



Electric Vehicle Transportation Center

Development of SWITCH-Hawaii Model: Loads and Renewable Resources

Mr. Paritosh Das
Mr. Deepak Chermakani
Dr. Matthias Fripp
University of Hawaii
Department of Electrical Engineering
2540 Dole St., Holmes Hall 483
Honolulu, HI 96822
E-mail: mfripp@hawaii.edu

Submitted to:

Dr. David Block
Florida Solar Energy Center
University of Central Florida
1679 Clearlake Road
Cocoa, FL 32922
E-mail: block@fsec.ucf.edu

Purchase Order Number: 291166
Report Number: HI-13-16
August 2016

The contents of this report reflect the views of the authors, who are responsible for the facts and the accuracy of the information presented herein. This document is disseminated under the sponsorship of the U.S. Department of Transportation's University Transportation Centers Program in the interest of information exchange. The U.S. Government assumes no liability for the contents or use thereof.



CONTENTS

Contents 1

Abstract 2

1 Introduction..... 2

2 SWITCH Model Overview..... 2

3 Study Years and Hours 3

4 New Power Plants..... 4

5 Existing Power Plants 5

6 Electricity Loads..... 5

 6.1 Baseline Electricity Loads for Oahu 5

 6.2 Load Forecast 5

7 Fuel Prices 6

8 Oahu Wind Resources 7

 8.1 Wind Resource Datasets..... 7

 8.2 High Resolution Wind Resource Maps..... 8

 8.3 Potential Wind Power Site Characterization/Selection 9

 8.3.1 Slope Exclusion 9

 8.3.2 Zoning Exclusion..... 9

 8.3.3 Off-shore Area Exclusion 11

 8.3.4 Unified Exclusion Map..... 11

 8.4 Micro-Siting of Wind Turbines..... 12

 8.4.1 Selection of Type of Turbine 13

9 Oahu Solar Resources..... 14

 9.1 Distributed PV..... 14

 9.1.1 Oahu Rooftop Inventory 15

 9.1.2 Calculating Maximum Distributed PV Capacity in Each OWITS Grid Cell 19

 9.1.3 Hourly Capacity Factor for Distributed PV Systems..... 20

 9.2 Central PV 21

 9.2.1 Central PV Site Selection..... 21

 9.2.2 Central PV Power Output 22

10 Conclusions 23

11 References 24

ABSTRACT

This report summarizes work done to configure the SWITCH power system model using data for the Oahu power system. SWITCH is a planning model designed to choose optimal infrastructure investments for power systems over a multi-decade period. Investments are optimized based on the cost of new renewable and conventional power plants and transmission capacity, and the hourly behavior of loads and potential renewable energy projects on several dozen sample days. SWITCH can also be run as a more detailed production cost model, which tests the performance of pre-selected investment plans using weather from hundreds of sample days.

Project 21 of the Electric Vehicle Transportation Center (EVTC) at the University of Central Florida will use the Oahu version of SWITCH to calculate the effects of several electric vehicle fleet configurations and charging strategies on the power system's design and operation. It will also be used to provide estimates of duty cycles for grid-to-vehicle and vehicle-to-grid applications, to support further analysis of battery degradation processes.

As described in this report, SWITCH has been configured with data on Oahu's existing power plants, potential new power plants, forecasted fuel prices, hourly electricity loads during 2007 and 2008, forecasted electricity loads (re-scaled versions of the 2007 and 2008 data) and hourly performance of potential renewable energy projects during this same period. Particular effort has gone into building a roof inventory dataset showing where rooftop photovoltaic systems could be sited, and a wind site dataset, showing where individual turbines could be placed on the island of Oahu, taking account of land use restrictions and topographic suitability. Potential sites for utility-scale photovoltaic systems have also been identified.

1 INTRODUCTION

This report summarizes a portion of the work conducted under Project 21 of the Electric Vehicle Transportation Center (EVTC) at the University of Central Florida: "Effect of Electric Vehicles on Power System Expansion and Operation." This project will use the SWITCH power system planning model (1) to perform several pieces of analysis:

- a) calculate the benefits of optimally-timed EV charging,
- b) identify the technical requirements and calculate costs of electric grid infrastructure to serve different types of vehicle fleets, and
- c) calculate battery duty cycles for grid-to-vehicle and vehicle-to-grid applications, to support further analysis of degradation processes.

Prior to this analysis, the project will configure the SWITCH model using Hawaii-specific data, and validate the production-cost component of SWITCH against previous results from GE MAPS, an industry-standard production-cost model.

This document reports work done to configure the SWITCH model using Hawaii data, particularly focusing on the datasets used to model hourly performance of potential wind and solar power systems and hourly electricity loads for non-vehicle applications. Later reports will discuss the configuration of SWITCH to match the inputs used for GE MAPS, validation of SWITCH against GE MAPS, and then the primary analysis listed above.

2 SWITCH MODEL OVERVIEW

SWITCH is an open-source, multi-period stochastic, linear optimization power system planning model previously developed by one of the principal investigators of this project (1). It consists of a lightweight, hourly production cost model nested within a multi-decade capacity

expansion model. SWITCH is designed to choose optimal plans for expansion and operation of power systems based on the hourly behavior of renewable resources, demand response, storage and conventional power plants. Figure 1 summarizes SWITCH’s structure and inputs. Readers who are unfamiliar with this model are advised to consult Fripp (1); this reference is available along with the model from <http://www.switch-model.org>.

SWITCH is a generic power system planning model which can be configured to identify optimal expansion and operation plans for any region. For this project, SWITCH has been initialized with the Hawaii-specific data needed for analyzing future energy scenarios on Oahu. In this report, we refer to the Hawaii-specific version of SWITCH as SWITCH-Hawaii.

More detailed information about the setup is provided in later sections.

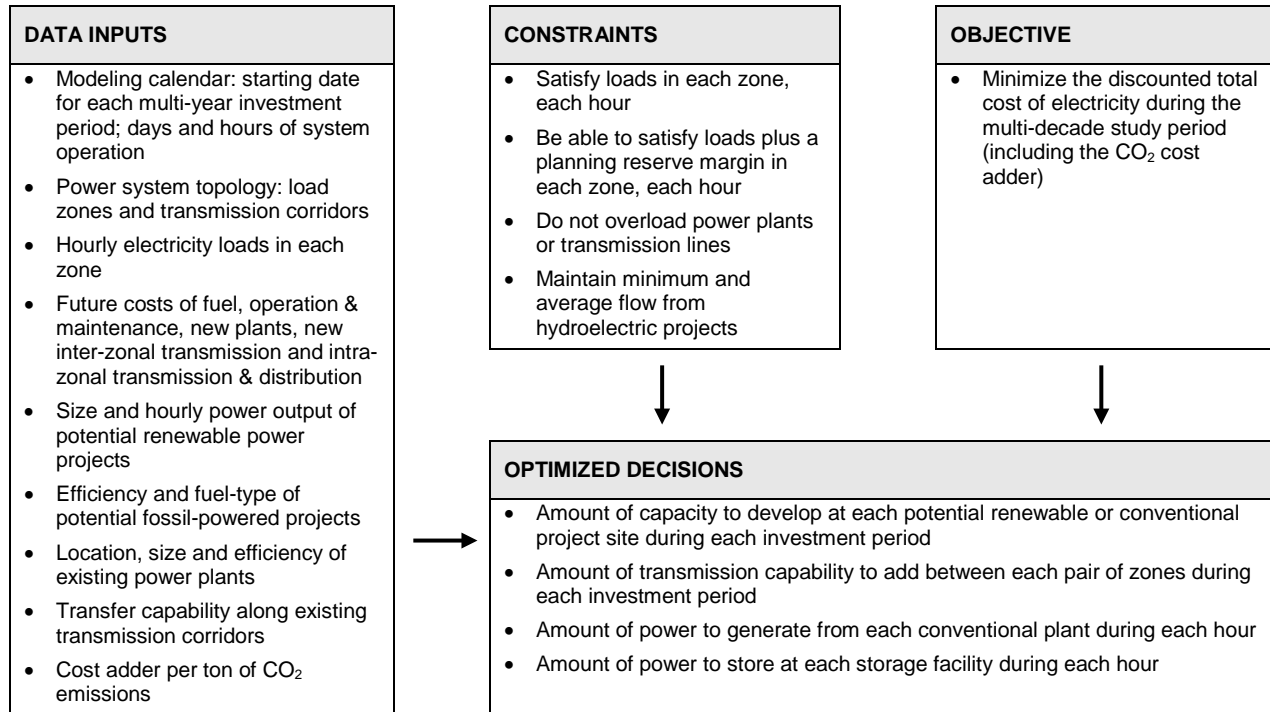


Figure 1. Inputs, constraints, objective, and decisions of the SWITCH model (1)

3 STUDY YEARS AND HOURS

For the initial setup, SWITCH-Hawaii has been configured to have four three-year investment periods, starting from 2015, 2018, 2021 and 2024. Twenty-four historical dates are chosen to represent environmental conditions during each investment period. These are made up of two dates for each month of the year: one date chosen to reflect typical operating conditions, and one representing a peak-load day for that month. The chosen historical dates were selected in such a manner that their collective average solar and wind output, very closely resemble the actual annual average. Conditions on the peak day are re-used for all four investment periods. This sampling method ensures that investment choices provide adequate reserves for the peak load day each period. All the historical dates are chosen from the years 2007 and 2008, as both renewable and load data are available for these years. This work relies heavily on finely time-resolved wind and solar resource datasets that were prepared for this period as part of the Oahu Wind Integration and Transmission Study (2).

During SWITCH’s investment optimization phase, fewer days are sampled than the actual

length of each investment period, so each sampled date is weighted to represent multiple study days during that investment period. For non-peak days, a weight represented by $(days_in_month - 1) * years_per_period$ is used, while for a peak-day, a weight of $years_per_period$ is used. For example, in the month of March, each sampled historical non-peak day was given a weight of 90 and a historical peak day was given a weight of 3, since the peak-day conditions occur less often.

4 NEW POWER PLANTS

The candidate technologies available to SWITCH for new generating capacity have been selected from the “Consolidated Unit Information Forms (UIFs)” section of Appendix K of Hawaiian Electric Companies’ 2013 Integrated Resource Planning (IRP) Report (3). The candidate technologies used in SWITCH-Hawaii are shown in Table 1.

Table 1. Technologies available for new generation capacity in SWITCH-Hawaii

| Label | Technology | Model | Fuel | Source ¹ |
|-------------------|---|---------------------------|-----------|---------------------|
| CCCT_LNG | combined cycle combustion turbine | GE LM6000 PG ² | LNG | Table L-7c |
| CCCT_Biodiesel | combined cycle combustion turbine | GE LM6000 PG | biodiesel | Table L-6c |
| Reciprocating | simple cycle reciprocating engine | 6x0 Wartsila 18V46 | biodiesel | Table K-2c |
| SCCT_LNG | simple cycle combustion turbine | GE LM6000 PG | LNG | Table L-7c |
| SCCT_Biodiesel | simple cycle combustion turbine | GE LM6000 PG | biodiesel | Table L-6c |
| CentralTrackingPV | single-axis tracking photovoltaic (utility scale) | | solar | Table B-3 |
| DistPV | distributed photovoltaic | | solar | Table B-1 |
| Wind | wind farm (utility scale) | | wind | Table A-1 |

¹All tables are located in the “Consolidated Unit Information Forms” section of Appendix K of Hawaii Energy Industries’ 2013 IRP Report (3).

²Note that the GE LM6000 PG can be used in either simple-cycle or combined-cycle modes.

Capital costs and technical characteristics (e.g., heat rate) for all technologies are taken from the UIFs, with one exception. Capital costs for distributed photovoltaic systems were estimated based on recent experience in the Hawaii market.

For each of these technologies (except DistPV), SWITCH’s $capital_cost_per_kw$ parameter for all years is set equal to the total capital cost reported in the UIFs, excluding T&D Interconnection and Power Plant Switchyard. The $connect_cost_per_kw$ parameter is set equal to the sum of T&D Interconnection and Power Plant Switchyard costs, divided by the rated capacity of each plant.

For the first five of these technologies (i.e. fuel based), the rated capacity is assumed to be the reported kW(net) value. For the sixth and seventh technologies (i.e. Central Tracking PV and Distributed PV), the rated capacity is the kW(dc) value (losses due to AC conversion and other factors are incorporated into the plant capacity factor, discussed below). For the eighth technology (i.e. Wind), the wind farm’s rated capacity is used as reported.

5 EXISTING POWER PLANTS

All existing power plant and generator data such as size (nameplate capacity), technology (prime mover, energy source), location, ownership, operational mode (baseload/cogeneration), and technical specifications (heat rate, operational year) for Oahu, were obtained from Form EIA-923 (4) and Form EIA-860 (5) which are the Energy Information Administration's power plant survey databases. The average heat rate of each existing power plant was determined by dividing the amount of fuel that consumed by the plant in 2012 by their net power generation during that period. The capital and the operating costs have been derived from the Consolidated Unit Information Forms in Appendix K (Supply-Side Resource Assessment) of the 2013 Integrated Resource Planning (IRP) Report, published by the Hawaiian Electric Companies (3) and from Table 8.2 of the 'Assumptions to the Annual Energy Outlook 2014' published by the U.S. Energy Information Administration (EIA) (6). (Capital costs are treated as sunk costs in SWITCH, and used only to derive a realistic levelized cost of power for the system; they do not affect investment or operation decisions.)

Existing wind and solar plants have also been modelled explicitly in SWITCH-Hawaii. These plants are assumed to have the same capital and operating costs as new plants of the same type. The siting of the existing wind power plants is described in Section 8.4.1.

6 ELECTRICITY LOADS

6.1 Baseline Electricity Loads for Oahu

The hourly electricity load data for the island of Oahu were obtained from the annual filings of FERC form 714 (7) for the years 2007 and 2008. The Federal Energy Regulatory Commission (FERC) collects hourly load data from all electric utilities with peak annual demand greater than 200 MW, including the Hawaiian Electric Company (HECO), Inc., which serves the island of Oahu.

6.2 Load Forecast

In the SWITCH model, each modeled day corresponds to one real, historical day; in SWITCH-Hawaii, these historical days come from the years 2007 and 2008. Historical loads are then scaled appropriately to represent future loads, based on the peak and average load in the historical year and future year.

The peak and average load forecast data for Oahu were obtained from Appendix E-2: Quantification of Peak Forecasts and Appendix E-1: Quantification of Sales Forecasts respectively, of the 2013 Integrated Resource Planning ("IRP") Report published by the Hawaiian Electric Companies (3). The dataset contains historical data and also has yearly forecasts for the planning period from 2014-2033. The IRP-2013 has generated forecasts for four scenarios, as shown in **Figure 2**, each of which is developed according to the assumptions of the potential future circumstances that they could operate. For the main SWITCH-Hawaii analysis, the scenario "Moved by Passion" has been selected to represent typical electricity forecast data. (Note that electricity loads in this scenario are the same as the "Stuck in the Middle" scenario.) This scenario assumes that the electricity demand grows at a moderate rate. Later, other sensitivity studies can be performed considering the other scenarios.

| Cost Driver | 1. Blazing a Bold Frontier | 2. Stuck in the Middle | 3. No Burning Desire | 4. Moved by Passion |
|--|--|--|--|--|
| Economic Conditions | Slow Growth | Moderate Growth | Strong Growth | Moderate Growth |
| Renewable Portfolio Standards (RPS) Energy Regulations | Raised: 2020 at 30% 2030 at 60% | Status Quo: 2020 at 25% 2030 at 40% | Lowered: 2020 at 20% 2030 at 30% | Status Quo: 2020 at 25% 2030 at 40% |
| Electricity Demand | | | | |
| ♦ Underlying Economic Sales & Peak | Low | Medium | High | Medium |
| ♦ Customer Renewable Self-Generation | Very High | Medium | Low | High |
| ♦ Energy Efficiency Portfolio Standards--EEPS | Exceeded 110% of Base | Partially Achieved 75% of Base | Partially Achieved 75% of Base | Achieved 100% of Base |
| ♦ Electric Vehicles | High | Medium | Low | Medium |
| Construction Cost Escalation Rate | General: 3% Renewables: 0% | General: 3% Renewables: 3% | General: 3% Renewables: 3% | General: 3% Renewables: 2% |
| Fuel Supply & Prices | | | | |
| ♦ Oil | High Forecast | Reference Forecast | Low Forecast | Reference Forecast |
| ♦ Biofuels | Low Forecast | High Forecast | High Forecast | High Forecast |
| ♦ LNG | High Forecast (high forecast for neighbor islands) | Reference (high forecast for neighbor islands) | Reference (high forecast for neighbor islands) | Reference (high forecast for neighbor islands) |
| Energy Incentives | Continue | Gradually phased out by 2016 | End 2014 | Continue |
| Greenhouse Gas Regulations | CO ₂ : \$100/ton | CO ₂ : \$0 | CO ₂ : \$0 | CO ₂ : \$25/ton |
| Operating Costs | Escalate at 1.87% | Escalate at 1.87% | Escalate at 2% | Escalate at 1.87% |

Figure 2. Scenarios in 2013 Integrated Resource Planning ("IRP") Report (3)

7 FUEL PRICES

Price forecasts for fuels such as biodiesel, bio-crude, high sulfur diesel, ultra low sulfur diesel (ULSD), liquefied natural gas (LNG), low sulfur fuel oil (LSFO), medium sulfur fuel oil (MSFO), and low sulfur industrial fuel oil (LSIFO) were obtained from Appendix E-11: Fuel Costs Forecast Data of the 2013 Integrated Resource Planning ("IRP") Report published by the Hawaiian Electric Companies (3). The forecast data have yearly price forecast for the period 2013-2033. For setting up the SWITCH model, the reference price forecasts have been used (in cases where only low and high price forecasts were available, the average of the two was selected as reference price). Low and high forecast scenarios can be used later for sensitivity analysis. The coal price forecasts were obtained from Appendix A: Table A1 published in the U.S. Energy Information Administration's (EIA's) Annual Energy Outlook 2014 (AEO2014) (8). The AEO2014 only reports coal price forecasts for the years 2020, 2014, 2020, and 2040. Using curve fitting, the data points were interpolated to determine the yearly coal price forecasts for the period 2013-2033.

8 OAHU WIND RESOURCES

8.1 Wind Resource Datasets

Hourly wind performance in SWITCH-Hawaii is based on wind resource datasets (9) developed by AWS Truepower for the Oahu Wind Integration and Transmission Study (OWITS). AWS Truepower developed these datasets for the Hawaiian Islands using the Mesoscale Atmospheric Simulation System (MASS) model. The dataset generated by this modeling reports wind speeds on a uniform grid with a horizontal resolution of 1km. The grid for the island of Oahu has dimensions of 131 by 127 and contains 16637 cells. A grid image for Oahu is shown in Figure 3. For each grid cell, the dataset includes a time series data file, showing wind speeds that would have occurred every 10 minutes during 2007 and 2008 (105408 records). The data fields present in the OWITS time series files are shown in Table 2. The latitude and longitude of each grid point can be found in the corresponding grid geo-reference files.



Figure 3. Oahu Grid Image [Grid dimensions = 131 x 127, 1km Grid Resolution]

For each the mesoscale grid point present in the grid, the 10 minute time series of wind speed was extracted and averaged for each hour. Data on annual average wind speeds for a finer 200-m grid were then used to introduce finer geographic scale into the dataset, as discussed in section 8.2.

Table 2. Data Fields present in each of the OWITS Time Series Data File

| Data Field | Description |
|-------------------|---|
| DATE | Date |
| TIME | Time (Greenwich Mean Time) |
| TSFC | Surface Skin Temperature (K) |
| PSFC | Surface Pressure (mb) |
| PCP | Accumulation Precipitation (mm or kg/m ²) |
| Q2M | Specific Humidity at 2M Above Ground Level (g/kg) |
| DSWRF | Downward Shortwave Radiation Flux (W/m ²) |
| DLWRF | Downward Longwave Radiation Flux (W/m ²) |
| T10 | Temperature at 10M Above Ground Level (K) |
| S10 | Wind Speed at 10M Above Ground Level (m/s) |
| W10 | Wind Direction at 10M Above Ground Level (Degrees) |
| T50 | Temperature at 50M Above Ground Level (K) |
| S50 | Wind Speed at 50M Above Ground Level (m/s) |
| W50 | Wind Direction at 50M Above Ground Level (Degrees) |
| T80 | Temperature at 80M Above Ground Level (K) |
| S80 | Wind Speed at 80M Above Ground Level (m/s) |
| W80 | Wind Direction at 80M Above Ground Level (Degrees) |
| T100 | Temperature at 100M Above Ground Level (K) |
| S100 | Wind Speed at 100M Above Ground Level (m/s) |
| W100 | Wind Direction at 100M Above Ground Level (Degrees) |
| T200 | Temperature at 200M Above Ground Level (K) |
| S200 | Wind Speed at 200M Above Ground Level (m/s) |
| W200 | Wind Direction at 200M Above Ground Level (Degrees) |

8.2 High Resolution Wind Resource Maps

In 2004, a project funded by Hawaiian Electric Company, Maui Electric Company, the Hawaii Department of Business, Economic Development & Tourism and the U.S. Department of Energy's National Renewable Energy Laboratory (NREL) prepared maps of annual wind speeds across the Hawaiian islands, with a spatial resolution of 200 meters (see Figure 4). These maps were developed using the MesoMap system and provide wind speeds at 30, 50, 70, and 100 meters above ground level (10) (11). The 200m horizontal resolution was considered sufficiently granular to reflect the influence of most terrain features and to identify specific locations for wind projects (9).

These maps provide greater detail on the spatial variation of wind speeds than the 1km time series datasets discussed in section 8.1. To take advantage of this additional detail, we extracted annual average wind speeds at 70 meter elevation from the 200m dataset, then calculated the ratio between the speed in each 200m cell and the average of all the 200m cells in the same 1km cell. This provided a scaling factor indicating which cells have higher and lower wind speeds within each 1km cell. We then multiplied the 1km time series data by the 200m speed scaling factor to obtain a 2-year time series for each 200m cell.

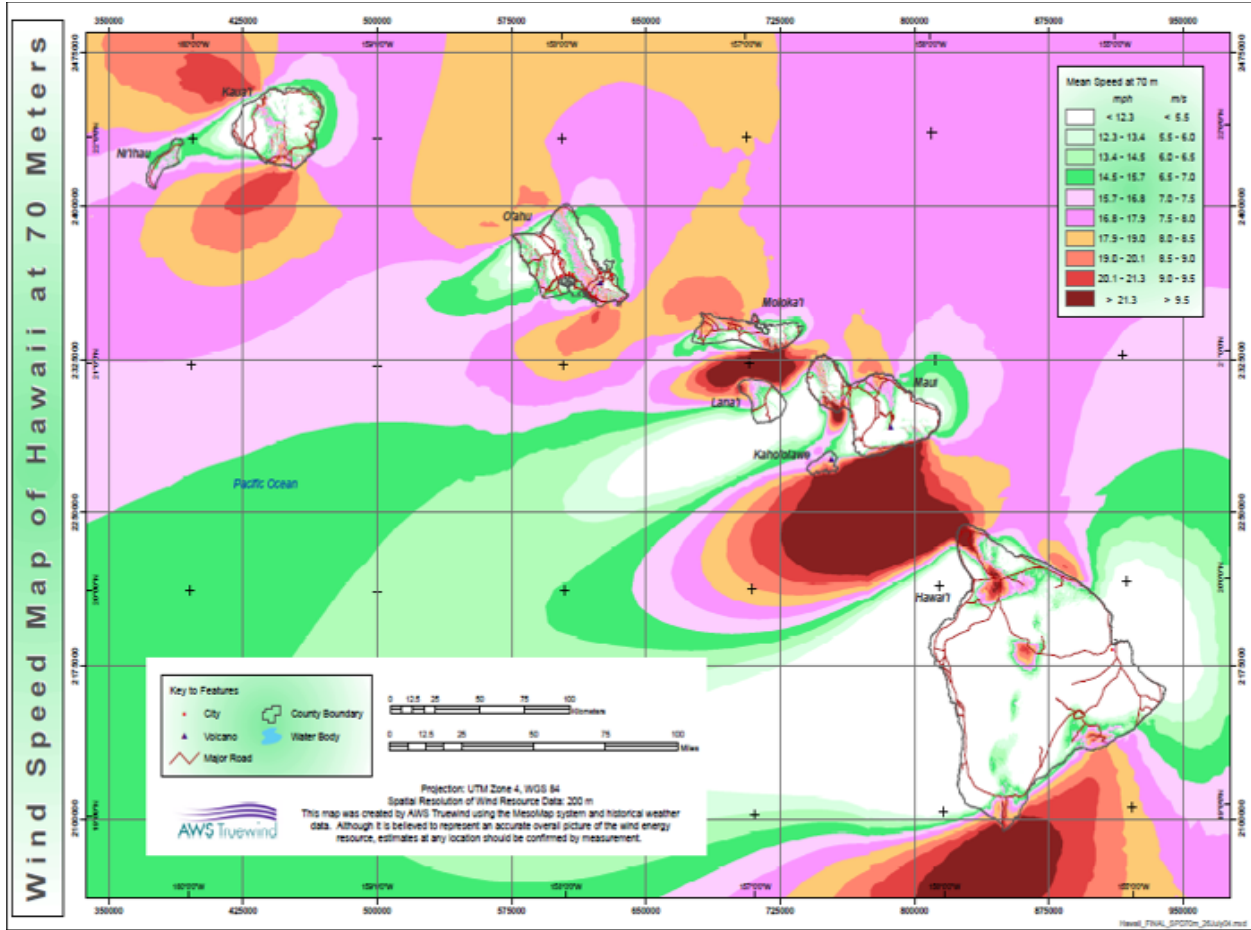


Figure 4. High-resolution wind resource map (as a jpeg image) for Hawaii (11)

8.3 Potential Wind Power Site Characterization/Selection

We used a Geographical Information System (GIS) approach to identify potential locations for wind turbines. We first developed various land exclusion criteria in the form of GIS maps. The various land exclusion criteria that were considered are listed in the following subsections.

8.3.1 Slope Exclusion

Digital elevation model (DEM) datasets for the island of Oahu were obtained from National Oceanic and Atmospheric Administration (NOAA) (12). All rasters have a spatial resolution of 10 meters and are in the ESRI grid format. These datasets were then analyzed in ESRI ArcGIS to show percent slope rise values. Areas having percent slope rise values greater than 20% were extracted to form the “Slope Exclusion Layer Map”. An additional buffer zone of 30 meters around the exclusion area was used to exclude boundary zones and small flat areas along ridge tops and valleys, where construction of a wind turbine would probably be infeasible.

8.3.2 Zoning Exclusion

We identified suitable zoning districts for wind power via the City and County of Honolulu Land Use Zoning GIS datasets (developed by the Department of Planning and Permitting, Honolulu Land Information System, City and County of Honolulu). Chapter 21 (Land Use Ordinance) of the Revised Ordinances of Honolulu (ROH) restricts zoning districts where wind turbines can

be sited. Table 3 lists the classification of zoning districts in the island of Oahu according to Article 3 of ROH Chapter 21 (13) (14) (15). Article 3 allows “Wind Machines” as a “Special accessory use” or via “Conditional use permit” only in Agricultural, Country, Business, Residential and some Industrial zones (AG-*, C, B-*, R-*, I-1, I-2 and IMX-1). However, Article 5 of ROH Chapter 21 (§21-5.700) prohibits wind turbines larger than 15 kW in business or residential zones, effectively excluding utility-scale wind farms from these zones (B-* and R-*). We judge that it is unlikely that wind farms would be developed in Limited Industrial District (I-1), Intensive Industrial District (I-2) and Industrial Mixed Use District (IMX-1) due to high land costs and difficulty integrating with existing land use and infrastructure, so we also exclude these from consideration. Accordingly, we allow wind turbines only in Restricted Agriculture District (AG-1), General Agriculture District (AG-2) and Country District (C) zones, as shown in Table 3.

An additional buffer of 300 meters was created around all excluded zones. This reduces the chance of conflicts with neighbors and respects the provision in ROH §21-5.700 that “All wind machines shall be set back from all property lines a minimum distance equal to ... the farthest vertical extension of the wind machine.”

Table 3. Oahu zoning district classifications and exclusions in SWITCH-Hawaii

| Zone Class | Zoning Description | Wind Farm Exclusion |
|-------------------|---|----------------------------|
| A-1 | Low-density Apartment District | excluded |
| A-2 | Medium-density Apartment District | excluded |
| A-3 | High-density Apartment District | excluded |
| AG-1 | Restricted Agriculture District | allowed |
| AG-2 | General Agriculture District | allowed |
| AMX-1 | Low-density Apartment Mixed Use District | excluded |
| AMX-2 | Medium-density Apartment Mixed Use District | excluded |
| AMX-3 | High-density Apartment Mixed Use District | excluded |
| Aloha | State Jurisdiction: Aloha Tower Project (Admin. by ATDC) | excluded |
| Apartment | Apartment Precinct (Waikiki Special District) | excluded |
| ApartmentMix | Apartment Mixed Use Subprecinct (Waikiki Special District) | excluded |
| B-1 | Neighborhood Business District | excluded |
| B-2 | Community Business District | excluded |
| BMX-3 | Community Business Mixed Use District | excluded |
| BMX-4 | Central Business Mixed Use District | excluded |
| C | Country District | allowed |
| F-1 | Federal and Military Preservation District | excluded |
| I-1 | Limited Industrial District | excluded |
| I-2 | Intensive Industrial District | excluded |
| I-3 | Waterfront Industrial District | excluded |
| IMX-1 | Industrial Mixed Use District | excluded |
| Kak | State Jurisdiction: Kakaako Community Development District (Admin. by HCDA) | excluded |
| MU | Mixed Use Precinct (Kakaako Special Design District) | excluded |
| P-1 | Restricted Preservation District | excluded |
| P-2 | General Preservation District | excluded |
| PU | Public Use Precinct (Kakaako Special Design District) | excluded |
| Pub | Public Precinct (Waikiki Special District) | excluded |
| R-10 | Residential District | excluded |
| R-20 | Residential District | excluded |
| R-3.5 | Residential District | excluded |
| R-5 | Residential District | excluded |
| R-7.5 | Residential District | excluded |

| | | |
|--------|--|----------|
| ResCom | Resort Commercial Precinct (Waikiki Special District) | excluded |
| ResMix | Resort Mixed Use Precinct (Waikiki Special District) | excluded |
| Resort | Resort District | excluded |
| WI | Waterfront Industrial Precinct (Kakaako Special Design District) | excluded |

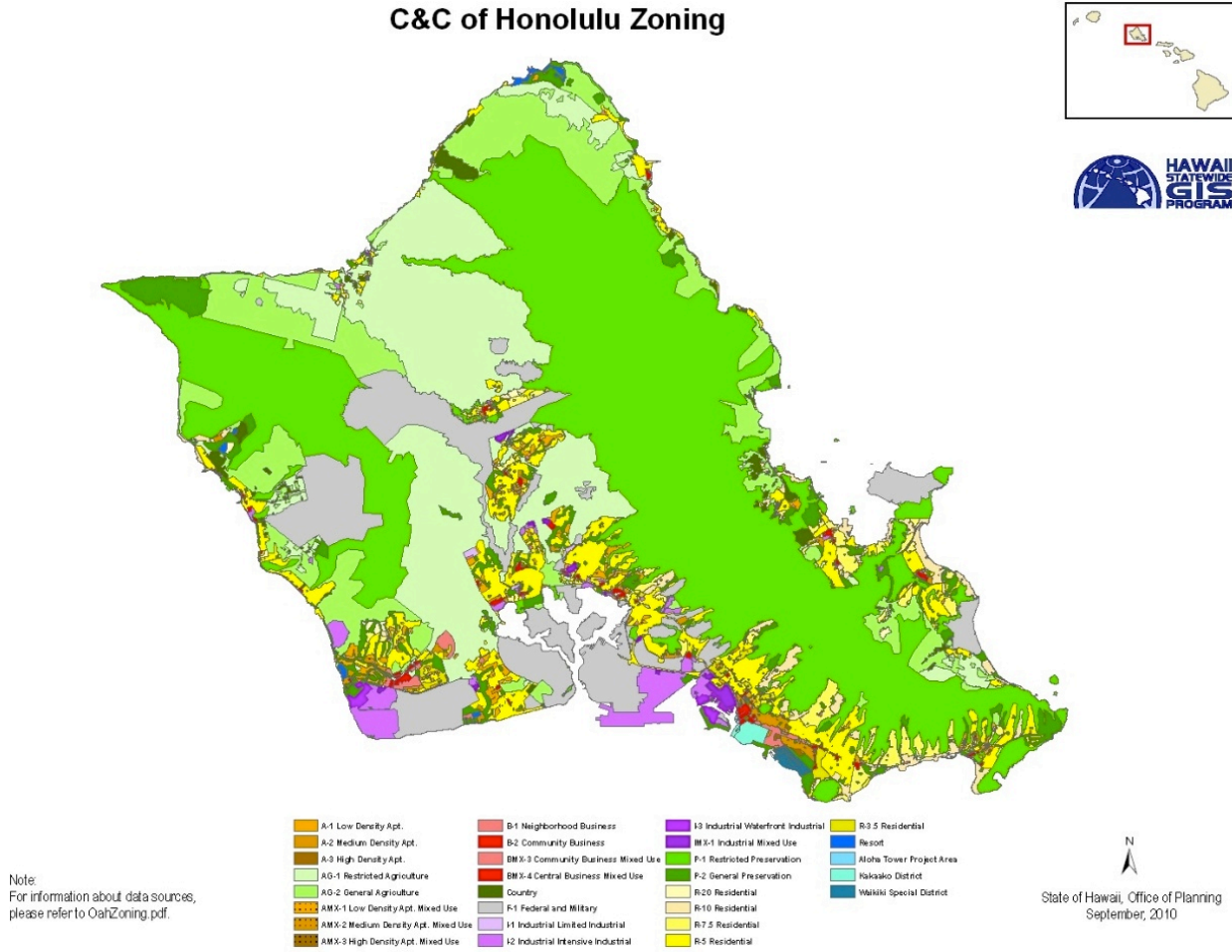


Figure 5. Map of City and County of Honolulu zoning districts (14)

8.3.3 Off-shore Area Exclusion

Hawaii’s off-shore areas are not generally seen as viable for near term development of wind power, due to deep water and sensitive marine habitat. Consequently, off-shore exclusion maps were created using GIS.

8.3.4 Unified Exclusion Map

All the above mentioned exclusion zone maps were merged into a single GIS dataset with horizontal resolution of 10 meters, as shown in Figure 6. This provides a complete inventory of land where wind farms could potentially be developed. It is unlikely that all of this land could be developed for wind farms, but this gives a starting point for considering how much may be attractive to develop. This map explicitly does not exclude areas with low wind speeds – those are left for selection or exclusion by SWITCH-Hawaii purely on their economic merits.

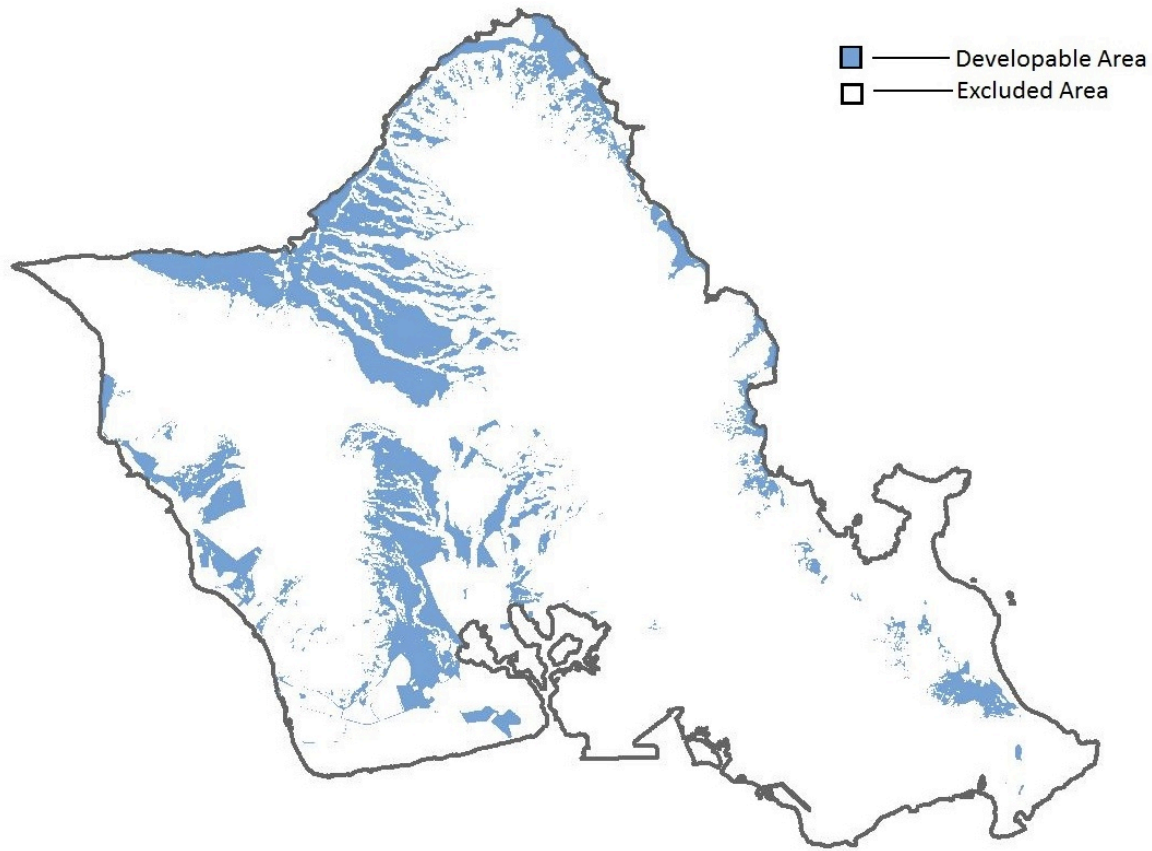


Figure 6. Map of potential wind energy development sites on Oahu

8.4 Micro-Siting of Wind Turbines

In order to estimate hourly power production from potential wind power projects, it is necessary to identify exactly where wind turbines might be placed. For this project we developed a simple script which placed wind turbines in suitable locations. This script scanned through all the developable cells of the GIS dataset, beginning in the northwest corner and scanning to the eastern edge, then moving one row south and repeating until the entire area had been scanned. Each time a developable cell was found, it was flagged to receive a wind turbine at its center, and then all other cells within 600 meters were excluded from consideration. This ensures that there is a minimum distance of 600 meters from the next selected grid cell. The minimum of 600 meters of distance between wind turbines is roughly 6 rotor diameters apart, assuming a wind turbine of rotor diameter of 100m. This resulted in 1,111 potential sites where wind turbines can be installed.

The most ideal arrangement of turbines in each region depends on the landscape topology and annual distributions of wind alignment (16). The approach used in this project neglects the opportunity to micro-site turbines on the windiest parts of complex terrain, or to align turbines to minimize wake effects in the prevailing winds. On the other hand, it also ignores the fact that some good sites may be unavailable for development, or some narrow sites may be oriented parallel to the wind, inducing excessive interference between turbines. We assume that these elements of conservatism and optimism roughly cancel out, so that the dataset provides a realistic representation of the amount of wind power that could be collected each hour.

A more detailed turbine placement process was used for the OWITS project (2); however,

turbine locations and wind farm output from that project were not placed in the public domain. Although our project did not undertake the detailed site modeling needed for exact turbine placement, we believe it nevertheless represents a significant advance in the Hawaiian wind production data available for research.

8.4.1 Selection of Type of Turbine

On the island of Oahu, only two wind farms are currently operational. These projects are operated by First Wind. The project details are summarized in Table 4. The type of turbines used in the two projects are 2.5 MW Clipper Liberty wind turbine (Kahuku wind farm) (17) and 2.3 MW Siemens SWT 2.3-101 wind turbine (Kawailoa wind farm) (18). Based on the above two model of turbines that have been used in Oahu for wind power generation, the 2.5MW Clipper Liberty turbines were selected as representative turbines for future wind power production.

Table 4. Existing wind farms in Oahu (17) (18)

| PROJECT | CAPACITY (MW) | TURBINES | TYPE OF TURBINE |
|--------------------|---------------|----------|------------------------------|
| Kawailoa Wind Farm | 69 | 30 | 2.3 MW Siemens (SWT-2.3-101) |
| Kahuku Wind Farm | 30 | 12 | 2.5 MW Clipper Liberty |

As per Clipper Liberty 2.5 MW wind turbine’s technical specifications (19) (20), the specification details of its 4 models are as shown in Table 5. Based on the annual average wind speed at the potential wind farm sites, the turbine models C89, C93 and C99 were selected to represent International Electrotechnical Commission (IEC) wind turbine classes I, II, III respectively.

Table 5. Clipper Liberty 2.5 MW Wind Turbine Specifications (19) (20)

| Model | C89 | C93 | C96 | C99 |
|--------------------|--------|--------|--------|--------|
| Wind Turbine Class | Ia | IIa | IIb | III |
| Rotor Diameter | 89m | 93m | 96m | 99m |
| Hub height | 80m | 80m | 80m | 80m |
| Rated Power | 2500kW | 2500kW | 2500kW | 2500kW |

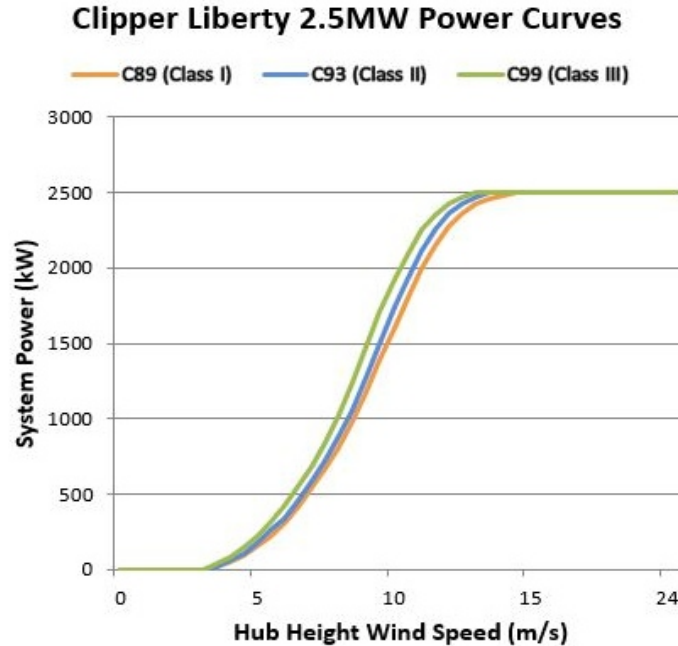


Figure 7. Clipper Liberty 2.5MW Wind Turbine Power Curve (20)

A wind site is classified as Class I if its annual average wind speed at hub height exceeds 8.5 m/s, Class II if it exceeds 7.5 m/s, and Class III if it is below 7.5 m/s. The turbine power curves for the selected turbine models (as shown in Figure 7) assigned to the different wind sites were used to calculate the hourly turbine power output at each potential turbine site. Typical wind turbine plant losses of 12.53% (as reported in the Consolidated Unit Information Forms present in Appendix K of Hawaiian Electric Companies' 2013 IRP report (3)), including array losses (8.0%), blade soiling losses (1.0%), control and turbulence losses (2.0%), and line losses (2.0%) were assumed.

In order to model the behavior of the existing wind farm projects in Oahu, potential turbine sites corresponding to the geographical location and equivalent capacity of the existing wind turbines were extracted from the list of potential wind turbine sites. The Kawaiiloa Wind Farm and the Kahuku Wind farm were equivalently replicated by 28 and 12 wind turbine sites respectively, with each wind power site having a rated power output of 2.5 MW. These existing wind farm sites are handled separately from potential sites for new turbines in SWITCH modeling.

Next, the selected 1,071 ($1,111 - 40 = 1,071$) potential wind turbine sites were clustered into 44 resource tranches based on annual average capacity factor and broad geographic location.

9 OAHU SOLAR RESOURCES

9.1 Distributed PV

To estimate hourly production from existing and potential distributed rooftop photovoltaic (PV) systems, we performed three steps:

1. create a rooftop inventory for all of Oahu based on roof images retrieved from the Google Static Map API;
2. calculate the potential rooftop PV capacity within each 1km cell of the weather datasets produced by the Oahu Wind Integration and Transmission Study (OWITS) (2); and

3. calculate the hourly capacity factor for a collection of PV systems uniformly distributed among all Oahu rooftops (i.e., a weighted average of the capacity factor in all the OWITS 1km cells).

This approach assumes that both existing and future distributed PV systems are uniformly distributed on available rooftops. This may not be exactly true, but we believe it gives a reasonable approximation of the performance of Oahu's geographically dispersed PV systems, within the limits of available data and forecasts.

The following sections describe these steps in more detail.

9.1.1 Oahu Rooftop Inventory

To identify locations where distributed rooftop photovoltaic systems could be installed, we used the Google Static Map API to download image tiles containing images of roof boundaries, and then used ArcGIS for further image analysis, such as converting images into polygons and calculating polygon areas.

The Google Static Map API (21) provides map tile images with user-specified resolution and features, via the HTTP protocol. This service is free for public use, up to 25,000 images per day, each of which can be up to 640 pixels square. The service uses a Mercator projection, with zoom levels ranging from 0 to 22 (22). Zoom level 0 corresponds to a 256×256 pixel tile showing the entire planet (180°W to 180°E and approximately 85°S to 85°N). Each higher zoom level doubles the resolution.

At a zoom level of 17 (corresponding to approximately 1 meter per pixel) or higher, Google Maps returns images with rooftop outlines. A sample URL of Google Static Map API is of this format: http://maps.googleapis.com/maps/api/staticmap?center=21.311605,-157.832865&zoom=17&size=320x320&sensor=true&visual_refresh=true&style=feature:all|element:all|visibility:off&style=feature:landscape.man_made|element:geometry.stroke|visibility:on

This URL returns the image shown in Figure 8, which contains 2-D outlines of all manmade buildings, in a square area centered at a latitude of 21.311695 and longitude of -157.832865.



Figure 8. Sample image returned by Google Static Map API

9.1.1.1 Retrieving Image Tiles

Internally, the Google Maps service divides the world into a number of tiles, each 256×256 pixels, that join seamlessly edge-to-edge and cover the whole planet. Different sized tiles are used at each zoom level. This coordinate system is not available for direct use via the Static Maps API. However, we achieved similar coverage for Oahu by requesting 256×256 pixel tiles whose central latitudes and longitudes were spaced exactly 256 pixels apart in the underlying coordinate system.

Locations in the tile coordinate system can be converted to latitude and longitude via

$$\begin{aligned}\text{longitude} &= 360^\circ \times \left(\frac{x}{2^z} - \frac{1}{2} \right) \\ p &= -2\pi \left(\frac{y}{2^z} - \frac{1}{2} \right) \\ \text{latitude} &= \frac{180^\circ}{\pi} \left(2 \operatorname{atan} e^p - \frac{\pi}{2} \right)\end{aligned}$$

where z is the zoom level and x and y are locations in tile coordinates. Integer values of x and y correspond to the corners of standard 256×256 pixel tiles, counting from 0 at the top and left edges to 2^z at the bottom and right edges. Fractional values of x and y correspond to locations within the standard 256×256 pixel tiles.

We used a python script to retrieve tiles from the Google Static Maps API, using the longitude and latitude formulas above, with $z=17$ and x and y set to a series of integer values spanning the island of Oahu. We retrieved tiles that were 360×360 pixels, centered at each integer (x,y) location, and then cropped to the central 256×256 pixels, to remove Google logos and metadata. (Note that this produces a seamless collection of centers are aligned with the corners of the standard Google grid.)

The images were then saved as png files, georeferenced to the Mercator projection using supplementary world files. A sample world file (for the image corresponding to Lat=21.6889972 and Lng=-157.70324707) is given as

```
1.19299213863
0
0
-1.19299213863
-17535953.6926
2421411.3718
```

The logic to obtain the six lines A, B, C, D, E, and F, of the World file is as follows:

$$A = \frac{c}{256 \times 2^z} \quad (\text{horizontal size of each image pixel, in meters})$$

$$E = -A \quad (\text{vertical size of each image pixel, in meters})$$

$$B = 0$$

$$D = 0$$

$$C = (x - 0.5) \times \frac{c}{2^z} - \left(\frac{c}{2} \right) \quad (\text{horizontal location of left edge of image, in meters})$$

$$F = - \left[(y - 0.5) \times \frac{c}{2^z} - \left(\frac{c}{2} \right) \right] \quad (\text{vertical location of top edge of image, in meters})$$

where c is the Earth's circumference (40030174 meters) and x , y , and z are as given above.

9.1.1.2 Converting Image Tiles to Roof Polygons

After retrieving a complete set of rooftop image tiles for Oahu, we imported all the tiles into a single mosaic raster in ESRI ArcGIS, and then converted the mosaic raster into a polygon shapefile, using ArcGIS's "Raster to Polygon" conversion tool. Since the roof outlines have non-zero thickness, this tool created compound polygons for each rooftop. These consist of one polygon aligned with the outer edges of the roof outline and another (acting as a hole) aligned with the inner edges of the roof outline. We then used ArcGIS's "Eliminate Polygon Part" tool to remove the inner polygons (ArcToolbox → Data Management Tools → Generalization → Eliminate Polygon Part → Eliminate contained parts only). When using this tool, we set the size option to 99%, to eliminate virtually any polygon that falls within each outer polygon.

The result of this processing was a shapefile with polygons corresponding to all roofs on the island of Oahu, as shown in Figure 9. These rooftop polygons cover roughly 5.04% of Oahu land area.

Note: an alternative approach would have been to retrieve the rooftop images from the Google Static Map API as filled polygons instead of outlines. However, the Google map API always draws these polygons in a partly transparent mode, against a background that varies depending on land use. The background uses similar color ranges to the rooftops, and this makes it difficult to systematically distinguish rooftop pixels from background pixels.

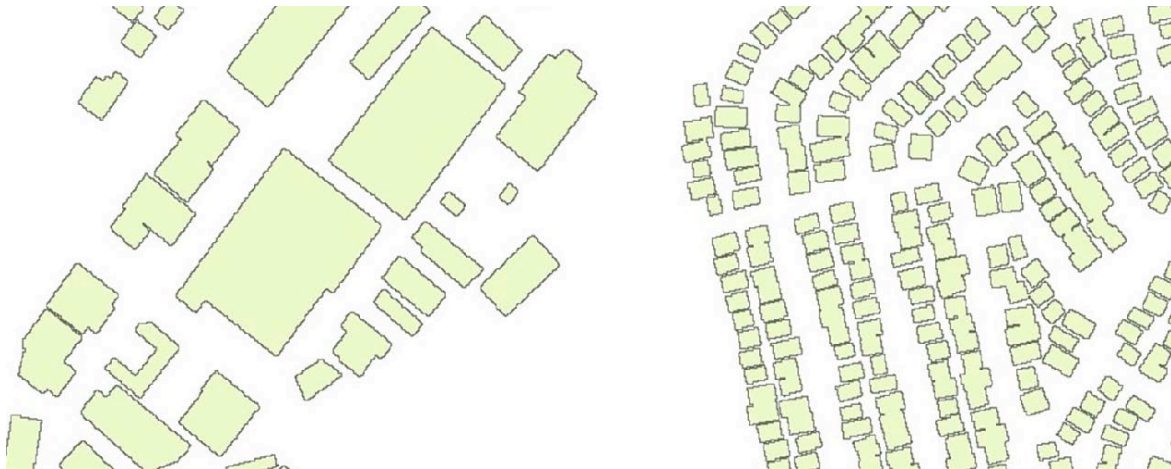


Figure 9. Section of Oahu rooftop polygon shapefile

9.1.1.3 Validation Against Census Data

In order to verify that the Google Maps API had a complete collection of rooftops (and possibly impute additional rooftops in areas where images were missing), we compared the rooftop data in our Google-based Oahu rooftop polygons shapefile with housing and population data from the U.S. Census.

We first used ArcGIS to identify the U.S. Census block in which each rooftop polygon (or portion of a polygon) fell. We then calculated the rooftop density (percent coverage) in each census block from our rooftop inventory, and compared this to population density (inhabitants per square meter) and housing density (number of units per square meter) from the U.S. Census block dataset.

Plots of these comparisons are shown in Figure 11 and Figure 12. Each point in these figures corresponds to one of Oahu's 8459 census blocks. For validation purposes, it is useful to consider three aspects of these figures:

First, there is something of a trend showing increasing roof coverage with increasing population or housing density, up to a saturation point around 50% roof coverage. This is roughly what we would expect – in lightly populated areas, housing units are mostly one or two stories and roof area scales up with population; however in densely populated areas, buildings get taller and roof density does not rise as quickly as population density.

Second, there are relatively few points that fall far below or to the right of the general trend. This indicates that there are no significant populated regions for which the Google Static Maps API failed to report roof area. Our original hypothesis (based on manual examination of some rural areas) was that Google may not have completed its rooftop footprint analysis for a significant portion of the island. We planned to identify these regions as outliers in Figure 11 or Figure 12 and then assign them estimated roof areas based on the trendline for the main body of data. However, this does not appear to be necessary.

Third, there are a significant number of points along the left axis of both figures. These are areas with significant roof coverage in the Google dataset but without any permanent population, e.g., commercial and industrial areas. This appears to indicate a significant advantage in using a direct image-based rooftop inventory. It would not be possible to estimate the size or location of these non-residential roofs via any other means that we have identified.

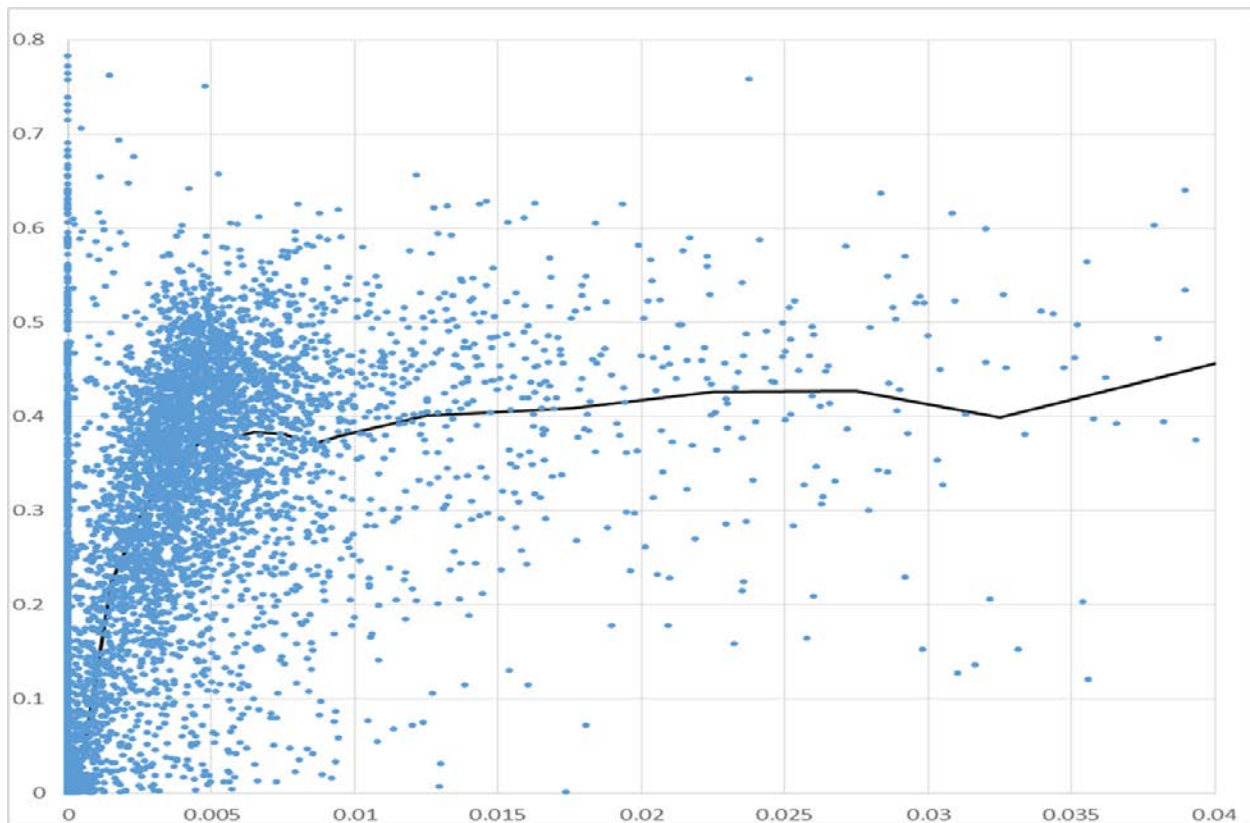


Figure 10. Rooftop coverage (%) vs. population density (people/m²) for Oahu census blocks

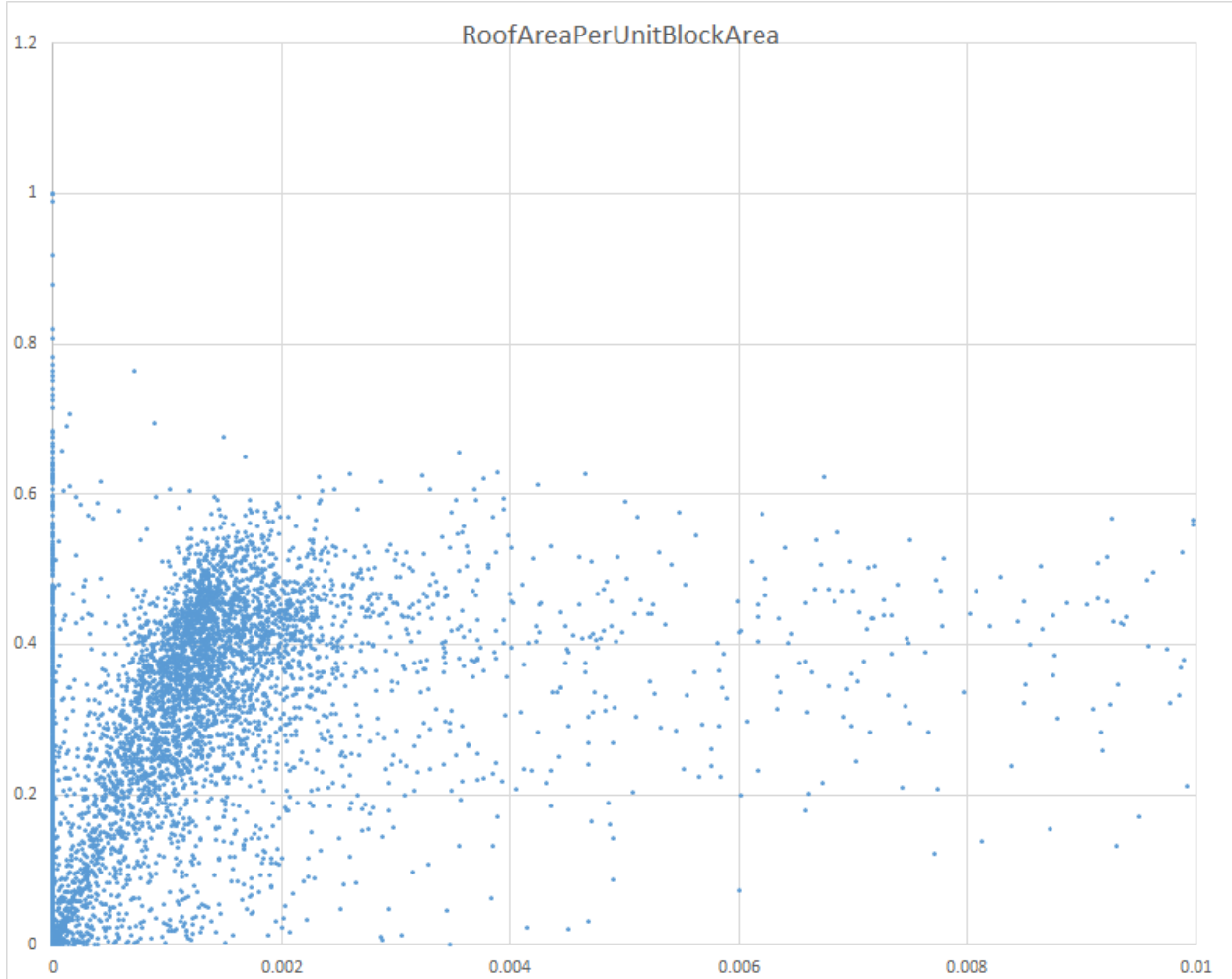


Figure 11. Rooftop coverage (%) vs. housing unit density (units/m²) for Oahu census blocks

9.1.2 Calculating Maximum Distributed PV Capacity in Each OWITS Grid Cell

We used the rooftop inventory discussed in Section 9.1.1 to estimate the maximum amount of distributed PV capacity that could be deployed in each of the 1km grid cells for which we have weather data from OWITS (2). This provides an upper limit for the amount of distributed PV that could be used in SWITCH-Hawaii. It also gives a rough estimate of the geographic distribution of distributed PV, assuming that actual deployment is proportional to the maximum (i.e. to roof area) in each region.

We first used ArcGIS to intersect the rooftop polygon layer with a layer corresponding to the OWITS grid cells, and calculated the amount of roof area within each OWITS cell.

In future work, this effort will be extended to subdivide the roof inventory by slope and azimuth, based on statistical sampling an analysis of Google rooftop images, Google Street View images or Microsoft Bing Birds Eye View (oblique) images. We will then calculate separately the irradiance on each tranche of PV orientation within each OWITS cell, and the corresponding power production.

However, for this preliminary analysis, we make a rougher approximation of the available roof inventory and the potential power production. We first assume that 15% of roofs are flat, and 85% are sloping, and that 50% of sloped roofs are oriented suitably to receive solar panels. We also assume that only 70% of all roof area could be covered by solar panels, due to inter-panel

spacing, shading, complex shapes, other utilities, etc. This gives us an estimate that the portion of roof area that could receive PV panels is equal to $(0.15 + 0.85 \times 0.5) \times 0.7 = 0.4$.

For this preliminary analysis, we also assume that PV production in any area is directly proportional to panel area and global horizontal irradiance (GHI). We found that this is a fairly good approximation, based on analysis of irradiance and PV production data prepared for the Hawaii Solar Integration Study (23). (As noted above, in future work we will directly estimate the effect of panel orientation on hourly power production.)

We define the rated capacity for each system as its DC power output under “peak” irradiance (1000 W/m^2), and we assume that the PV panels have DC efficiency of 12%. This gives a simple model for calculating the maximum PV capacity in each OWITS grid cell i :

$$[\text{maximum PV capacity (MW)}]_i = [\text{roof area (m}^2)]_i \times 0.4 \times 0.12 \times 1000 \text{ W/m}^2 \times 10^{-6} \text{ W/MW}$$

The maximum amount of distributed PV that can be installed on the entire island is given by

$$[\text{maximum Oahu PV capacity (MW)}] = \sum_{i \in \text{cells}} [\text{maximum PV capacity (MW)}]_i .$$

9.1.3 Hourly Capacity Factor for Distributed PV Systems

As noted in section 9.1.2, we are currently using the simplifying assumption that PV production in any area is directly proportional to global horizontal irradiance (GHI). With this assumption, the capacity factor for distributed PV systems in each OWITS cell (i) during each hour (h) is given by

$$\begin{aligned} & [\text{capacity factor (\%)}]_{i,h} \\ &= \frac{[\text{actual power}]_{i,h}}{[\text{rated power}]_i} \\ &= \frac{[\text{installed capacity}]_i \times [\text{GHI (W/m}^2)]_{i,h} \times \eta_s \times \eta_L}{[\text{installed capacity}]_i \times [1000 \text{ W/m}^2] \times \eta_s} \\ &= \frac{[\text{GHI (W/m}^2)]_{i,h}}{1000 \text{ W/m}^2} \times \eta_L \end{aligned}$$

Where η_s is the solar panels’ efficiency in converting sunlight to DC power and η_L is the system’s net efficiency in all other conversions (DC power to end-use). We assume that η_s is 12% and η_L is 91.6%. The value for η_L is the product of all efficiency factors listed in the “Energy Loss Factors” sub-table in Table B-1 of Appendix K of the 2013 IRP Report (3), except for availability, which is incorporated elsewhere in SWITCH. These factors include DC-AC conversion (97%), soiling (99%), shading (98%), auxiliary load (99.9%), DC cabling (98.5%), mismatch (99%) and AC wiring (99.9%).

Under the further assumption that both existing and future distributed PV systems are uniformly distributed on available rooftops, the capacity factor for the complete collection of distributed PV systems on Oahu can be calculated as the weighted average of capacity factors in individual OWITS cells:

$$[\text{capacity factor}]_h = \frac{\sum_{i \in \text{cells}} [\text{maximum PV capacity (MW)}]_i \times [\text{capacity factor}]_{h,i}}{\sum_{i \in \text{cells}} [\text{maximum PV capacity (MW)}]_i}$$

Under these assumptions, the entire distributed PV fleet can be modeled as if it were a single project, with a single time series of hourly capacity factors ($[\text{capacity factor}]_h$) and a single maximum PV capacity ($[\text{maximum Oahu PV capacity (MW)}]$). For this project, however, we divide the distributed PV into two collections, one representing the existing PV plants, and one representing potential future PV plants. The total amount of existing PV is subtracted from the maximum possible capacity, to determine the amount of additional distributed PV that can be installed on Oahu. Both existing and new PV have the same hourly capacity factor.

In future work – with transmission constraints, more detail on the location of existing PV arrays, or the option of optimizing the location where new distributed PV is installed – the fleet will be divided into a number of separate projects with different capacity limits and capacity factors.

9.2 Central PV

9.2.1 Central PV Site Selection

In order to identify potential sites/locations for central PV projects, the same screening procedure was used as for wind in 8.3 (slope exclusion, zoning exclusion, off-shore area exclusion). Areas in Oahu which have the potential for Central PV plants are shown in Figure 6. This map was then overlaid with the 1km OWITS mesoscale grid to determine the exact 1km grid cell location of potential central PV sites. Figure 12 shows the 1km grid cells where potential Central PV stations can be developed. A total of 731 1km grid cells were identified with potential for Central PV stations. Each of these was modeled as a potential project in SWITCH-Hawaii, with a capacity limit based on available land area within the 1km grid cell and the land use requirements given in table B-3 of Appendix K of Hawaii Energy Industries' 2013 IRP Report (3).

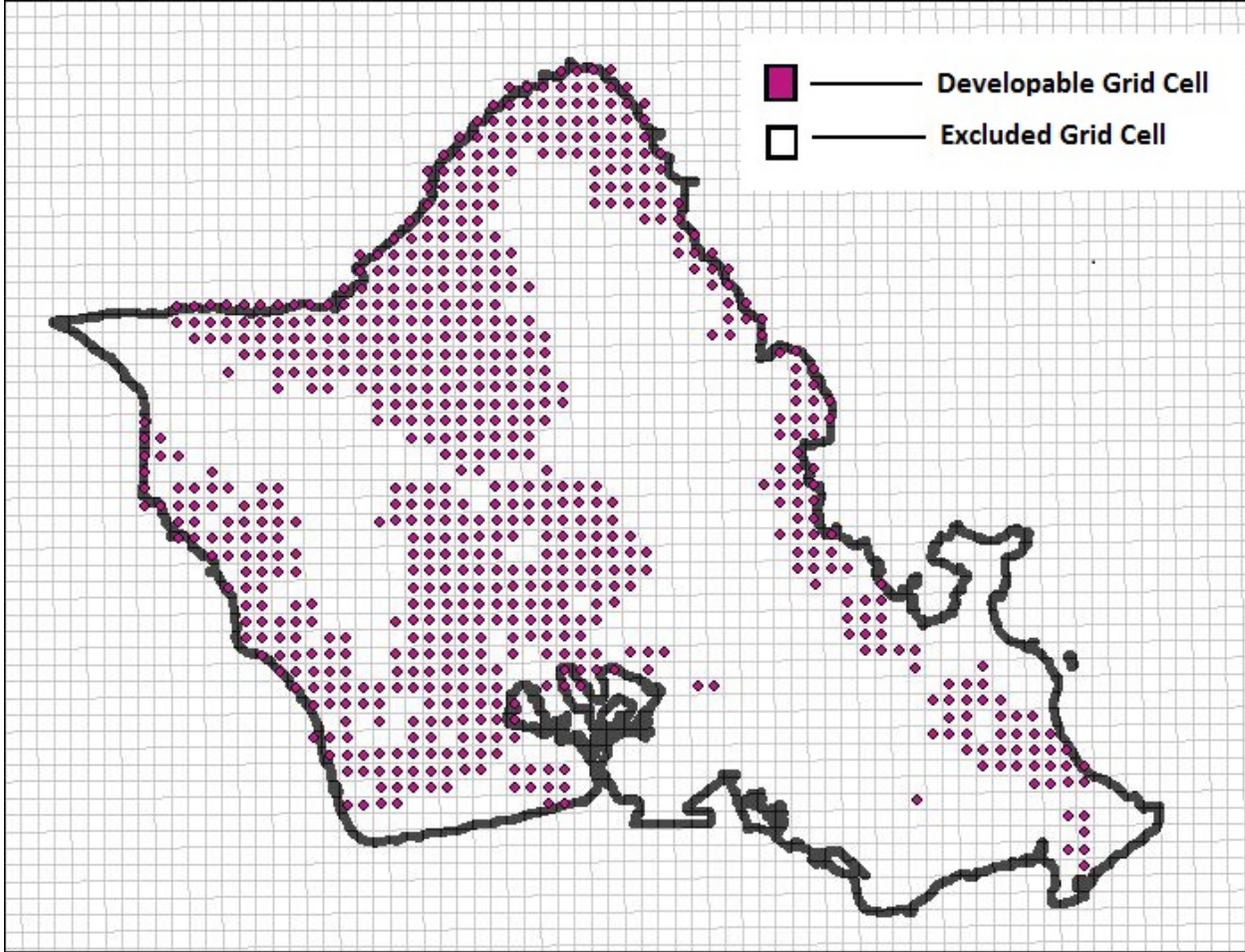


Figure 12. Potential Central PV station locations on Oahu

9.2.2 Central PV Power Output

Since we use single-axis tracking technology for the Central PV Stations, we use this technology to report the capacity factor for each hour, for each of the cells identified as Central PV projects.

Note that unlike the distributed PV projects, the Central PV technology treats each individual cell as a separate project.

For each of these identified cells, and for each hour, we calculate the ϕ_angle , δ_angle , ω_angle , z_angle , \cos_z , \cos_i , and I_0 , using the formulae used in (24).

We then calculate the value of clear-sky-index (k_T) = GHI / I_0 . Note that the closer k_T is to unity, the lesser the effect of clouds.

From this value of k_T , we find the diffused irradiance based on 3 cases mentioned in (24).

$$\begin{aligned} \text{Diffused_Irradiance} &= GHI * (1 - 0.09 * k_T) \text{ IF } (k_T \leq '0.22') \\ &= GHI * (0.9511 - 0.16 * k_T + 4.388 * \text{pow}(k_T, 2) - 16.638 * \text{pow}(k_T, 3) + \\ &\quad 12.336 * \text{pow}(k_T, 4)) \text{ IF } (k_T > '0.22' \text{ AND } k_T \leq '0.8') \\ &= GHI * 0.165 \text{ OTHERWISE} \end{aligned}$$

The above code is an implementation of these 4 cases.

From this, we know that the value of

$$DNI * \cos_z = GHI - \text{Diffused}, \text{ so we know that } DNI = (GHI - \text{Diffused}) / \cos_z$$

$$\text{We now set } \text{Tracking_radiation_panels} = \text{Diffused} + \cos_i * DNI$$

We now set $\text{Capacity_factor_panels} = 0.001 * \text{Tracking_radiation_panels}$

We finally incorporate losses by saying that $\text{capacity_factor_panels} = 0.896 * \text{Capacity_factor_panels}$

Note that this ratio of 0.896 is obtained by multiplying all energy-loss-factors (except “Availability”) from the Energy Loss Factor sub-table in Table B-3 of the Appendix K of the 2013 IRP Report (3).

To ensure that capacity factor never goes above 1, we limit it to 1 wherever it exceeds 1.

10 CONCLUSIONS

The work described in this report has laid the foundation for more advanced studies of Oahu’s power system using the SWITCH planning and production cost model. The key datasets for this work have been assembled, showing mainstream expectations of future equipment costs and electricity demand, as well as hourly behavior of electricity loads and potential renewable energy projects. Future work will add spinning reserve modeling capabilities to SWITCH, and then validate SWITCH’s production cost component against previous work using the industry-standard GE MAPS model. Subsequent work will use SWITCH to study the interaction of electric vehicles with the power system, identifying how different fleet types and charging strategies will affect the design of the power system and the cost of electricity and transport. Future work will also show the types of charging cycles that electric vehicles will undergo if they are charged under business-as-usual or optimal scenarios, and using grid-to-vehicle or vehicle-to-grid capabilities. In addition, SWITCH will be extended in the future to model other Hawaiian islands, using the same data sources as have been described in this report.

11 REFERENCES

1. Fripp M. Switch: A Planning Tool for Power Systems with Large Shares of Intermittent Renewable Energy. 2012; 46(11): p. 6371–6378.
2. Corbus D, Schuerger M, Roose L, Strickler J, Surlis T, Manz D, et al. Oahu Wind Integration and Transmission Study: Summary Report. Golden, Colorado: National Renewable Energy Laboratory; 2010.
3. Hawaiian Electric Companies. 2013 Integrated Resource Planning Report. ; 2013. Report No.: Docket No. 2012-0036.
4. U.S. Energy Information Administration (EIA). [Online]. [cited 2014 November 5. Available from: <http://www.eia.gov/electricity/data/eia923/>].
5. U.S. Energy Information Administration (EIA). [Online]. [cited 2014 November 5. Available from: <http://www.eia.gov/electricity/data/eia860/>].
6. Assumptions to the Annual Energy Outlook 2014. ; 2014.
7. Federal Energy Regulatory Commission (FERC). Form No. 714 - Annual Electric Balancing Authority Area. ; 2014.
8. U.S. Energy Information Administration (EIA). Annual Energy Outlook 2014 (AEO2014). ; 2014. Report No.: DOE/EIA-0383(2014).
9. AWS Truepower L. Development of Regional Wind Resource and Wind Plant Output Datasets for the Hawaiian Islands. ; 2010. Report No.: NREL/SR-550-48680.
10. AWS Truewind, LLC. Department of Business, Economic Development and Tourism (DBEDT), Hawaii State Energy Office. [Online].; 2004 [cited 2014 November 5. Available from: http://energy.hawaii.gov/wp-content/uploads/2011/10/WindEnergyResourceMapsHawaii_AWSTruewind_2004.pdf].
11. AWS Truewind, LLC. Hawaii State Energy Office Publications. [Online]. [cited 2014 November 5. Available from: http://energy.hawaii.gov/wp-content/uploads/2011/10/Hawaii_FINAL_SPD70m_26July04.pdf].
12. National Oceanic and Atmospheric Administration (NOAA). National Oceanic and Atmospheric Administration (NOAA). [Online].; 2007 [cited 2014 November 5. Available from: <https://data.noaa.gov/dataset/digital-elevation-models-dems-for-the-main-8-hawaiian-islands>].
13. Revised Ordinances of Honolulu (ROH) Chapter 21 - City and County of Honolulu. Article 3 Sec. 21-3.10 - Establishment of Zoning Districts and Zoning District Regulations. [Online]. [cited 2014 November 5. Available from: <http://www.honolulu.gov/rep/site/ocs/roh/ROHChapter21a3.pdf>].
14. City and County of Honolulu. OahZoning Metadata. [Online].; 2014 [cited 2014 November 5. Available from: <http://files.hawaii.gov/dbedt/op/gis/data/oahzoning.pdf>].
15. Revised Ordinances of Honolulu (ROH) Chapter 21 - City and County of Honolulu. Article 5 Sec 21-5.700 - Specific Use Development Standards. [Online]. [cited 2014 November 5. Available from: http://www.honolulu.gov/rep/site/ocs/roh/ROHChapter21a4_6.pdf].
16. Richard J. A. M. Stevens DFGaCM. Large Eddy Simulation studies of the effects of alignment and wind farm length. 2014.
17. Kahuku Wind Farm - Fact Sheet. [Online]. [cited 2014 November 5. Available from: <http://www.firstwind.com/wp-content/uploads/2014/01/Kahuku-Fact-Sheet-2014.pdf>].
18. Kawaihoa Wind Farm - Fact Sheet. [Online]. [cited 2014 November 5. Available from: <http://www.firstwind.com/wp-content/uploads/2014/01/Kawaihoa-Fact-Sheet-2014.pdf>].
19. Mikhail A. Distributed Generation Drivetrain for High-Torque Wind Turbine Applications. ; 2005. Report No.: CEC-500-2011-002.
20. Idaho National Laboratory. Idaho National Laboratory. [Online]. [cited 2014 November 5. Available from: <https://inlportal.inl.gov/portal/server.pt?open=512&objID=424&PageID=3993&cached=true&mode=2&userID=1829>].
21. Google, Inc. Static Maps API V2 Developer Guide. [Online].; 2014 [cited 2014 12 18. Available from: <https://developers.google.com/maps/documentation/staticmaps/>].
22. Google, Inc. Google Maps JavaScript API V3 Reference. [Online].; 2014 [cited 2014 12 18. Available from: <https://developers.google.com/maps/documentation/javascript/reference>].
23. Piwko R, Roose L, Orwig K, Matsuura M, Corbus D, Schuerger M. Hawaii Solar Integration Study: Solar Modeling Developments and Study Results. Golden, Colorado: National Renewable Energy Laboratory; 2012. Report No.: NREL/CP-5500-56311.

24. Duffie JA, Beckman WA. Solar Engineering of Thermal Processes. 2nd ed. New York: John Wiley and Sons, Inc.; 1991.
25. Fripp M. Online Supporting Information for Switch: a planning tool for power systems with large shares of intermittent renewable energy. Environmental Science & Technology. 2012; 46(11).
26. Hawaiian Electric Companies. 2013 Integrated Resource Planning Report. Honolulu.; 2013. Report No.: http://www.hawaiianelectric.com/heco/_hidden_hidden/Renewable-Energy/2013-IRP-Report-Chapters-and-Appendices.